SECTION II - CHAPTER 4

4.1 Chapter Introduction

This chapter deals with the biosynthesis of silver nanoparticles (AgNPs) from aqueous leaf-extract of an aquatic fern, *Salvinia molesta* (AES). It is worth to mention here that we have developed a new inexpensive photo-induced, fastest green route for the rapid biosynthesis of AgNPs using AES. The developed process was able to synthesize the AgNPs within 20 sec without using any instrumental support. Synthesized AgNPs were characterized through UV–visible spectroscopy, Fourier Transform Infrared (FTIR) spectroscopy, Field Emission Scanning Electron Microscopy (FESEM), Energy Dispersive X-Ray spectroscopy (EDX), High Resolution Transmission Electron Microscopy (HRTEM), Atomic Force Microscopy (AFM) and X-ray diffraction (XRD) analysis. Antimicrobial potential of prepared AgNPs was evaluated through disk diffusion method. On the basis of instrumental characterization and results, a probable mechanism for AgNPs synthesis and stabilization was also proposed.

4.2 Why AgNPs and their herbal biosynthesis?

Green synthesis of AgNPs has received considerable attention due to their unique properties and wide applicabilities [Ahmad et al., 2010; Huang et al., 2011; Sharma et al., 2009]**.** AgNPs have also been investigated for their antimicrobial and wound healing properties [Wen et al., 2015]. AgNPs can be synthesized through chemical, physical and biological synthesis routes [Rao and Pariya, 2013]. Although, chemical and physical are much popularized yet the expensiveness, toxicity of used reductants as well as aggregation problem with synthesized of nanoparticles limits the applicability of physical and chemical synthesis processes [Gade et al., 2014]. Recently, biological or green synthesis approach is grooming as an alternative method to avoid the problems and limitations associated with physical and chemical approaches [Bozanic et al., 2010; Saxena et al., 2012]. Till now various green routs for nanoparticle synthesis using bacteria, fungi, algae and plant extracts have been

reported [Mandal et al., 2006; Mukherjee et al., 2001; Xie et al., 2007; Lukman et al., 2011]. Moreover, synthesis of nanoparticles using plant extracts is more advantageous over other green route because it is simple, user friendly and less time consuming approach thus opted in current study [Clark 1999]. Some plant extract are able to synthesize the nanoparticles because they contains various phytochemicals such as phenol derivatives, flavonoids, proteins, terpenoids and reducing sugars. These phytochemicals of herbal extracts can act as both the reducing agent as well as capping agent required for the synthesis and stabilization of nanoparticles [Thakkar et al., 2010; Bulut et al., 2009].

Salvinia molesta and *Tamarindous indica* were selected for biosynthesis of AgNPs from eighteen screened plants as enlisted in *Table 4.1:*

Table 4.1 Name of screened plants with the reported results on their potency to synthesize AgNPs from their herbal extracts

Sr. No.	Name of the screened plant	Potential for AgNPs synthesis
1	*Terminalia arjuna*	Activity Absent
2	*Kigelia africana*	Activity Absent
3	*Eucklypata globosa*	Activity Absent
4	***Salvinia molista***	***Activity Present***
5	*Musa paradisiaca*	Activity Absent
6	*Ageratum conyzoides*	Activity Absent
7	*Ageratina adenophora*	Activity Absent
8	*Cassia tora*	Activity Absent
9	*Sesabinia asculanta*	Activity Absent
10	*Blainvillea acmella*	Activity Absent

11	*Chloris barbata*	Activity Absent
12	*Conyza bipinnatifida*	Activity Absent
13	*Imperata cylindrica*	Activity Absent
14	*Malvastrum coromandelianum*	Activity Absent
15	***Tamarindous indica***	***Activity Present***
16	*Typha angustata*	Activity Absent
17	*Blumea ariantha*	Activity Absent
18	*Cassia obtusifolia*	Activity Absent

4.3 About *Salvinia molesta*

Salvinia molesta is a floating fern, commonly known as *'Giant Salvinia'*. It is mainly native to 'South America' but also found in 'India' as an exotic weed [D. Oliver et al., 1993]. It normally grows rapidly as dense mats over the surface of still water. Overgrowth of *Salvinia molesta* hampers the oxygen exchange between environment and water and makes the water unsuitable for aquatic animals. Salvinia is being globally considered as one of the most troublesome aquatic weed due to its massive hazardous effects on aquatic environment [Mukherjee et al., 2014]. *Fig 4.1* shows the plant of *Salvinia molesta* in its native aquatic environment.

Fig. 4.1* Plant of *Salvinia molesta

4.4 Materials

For the biosynthesis of AgNPs, the only chemical used was $AgNO_3$ and it was procured from Merck (Mumbai, India). MHA, MHB and NA media (Hi-Media, Mumbai, India) were utilized for the assessment of antibacterial efficacy of AgNPs and for maintaining bacterial cultures respectively. Fresh leaves of fern, *Salvinia molesta,* were collected from Department of Botany, Banaras Hindu University, Varanasi, India. Collected leaves were further processed in lab to prepare leaf extract.

4.3 Methods

4.5.1 Preparation of aqueous extract from *Salvinia molesta* leaves (AES)

After collection the leaves of the *Salvinia molesta* were washed thoroughly with deionized water and then air dried for 3 h at room temperature under shade condition to remove extra water. Thereafter, 20 g of small pieces of the chopped leaves were boiled for 5 min at 100°C in 100 mL of deionized water. After boiling the solution was cooled down up to room temperature and then AES was collected through filtration via 'Whatman filter paper No 1'. The collected AES was stored at 4°C and utilized for experimentation within 3 days of preparation. *Fig. 4.2* represents the freshly prepared AES.

Fig 4.2 Aqueous extract of *Salvinia molesta* (AES)

4.5.2 Bio-synthesis of AgNPs using AES

Experiments were started with two sets of reaction mixtures each having 10 mL of 1 mM $AgNO_3$ solution and 2.5% (v/v) AES inoculum dose at pH 7.0. The amount of AES inoculum dose and $AgNO_3$ concentration were arbitrarily selected for starting experiments. The first set of reaction mixture was kept in direct sun light while other was kept in dark condition in incubator at same temperature as for first set in ambient environment. For the first set, environmental temperature was 36 °C and solar intensity was 440 lux respectively. Reaction mixture of first set was found to exhibit rapid color change within 20 sec of reaction time whereas reaction mixture in second set showed no significant change in color up to 12 h reaction time, which indicate that the AgNPs biosynthetic reaction was photocatalytic in nature. This Photocatalytic nature of the process was also confirmed by UV-visible spectrophotometeric (Evolution 201, Thermo Scientific) screening the samples withdrawn from both the reaction mixtures for the presence of characteristic SPR band of AgNPs. After confirming the photocatalytic nature of the process, further all experiments of AgNPs synthesis were conducted in direct sunlight in order to optimize the process parameters using one factor at a time approach. The process parameters were screened in the following range; duration of sunlight exposure from 0-40 min, AES inoculum dose from 2.5%-12.5% (v/v) and $AgNO_3$ concentration from 1.0 mM to 10 mM. During optimization, the temperature and pH were not taken in account as process parameters for keeping the developed process closer to the native environmental conditions and to avoid any instrumental or chemical support. Therefore, experiments were conducted at normal ambient temperature (35 ± 2°C) and neutral pH. After process optimization, the synthesized AgNPs were purified and collected. For purification, the reaction mixture was centrifuged at 10,000 rpm for 10 min and pallet was resuspended in deionized double distilled water followed by recentrifugation at 10,000 rpm for 10 min further

same step was reperformed with acetone. This process was repeated four times to eliminate the uncoordinated bio-molecules and dry mass of AgNPs was collected after lyophilization of aqueous suspension.

4.5.3 Characterization of AgNPs

The biosynthesis of AgNPs was initially confirmed and monitored by UV–visible spectroscopy through measuring the characteristic optical properties of AgNPs in the range of 300 to 700 nm. The involved functional groups in biosynthesis and stabilization of AgNPs were screened through FTIR in the range of 4000–400 cm^{-1} using Varian 3100 FTIR spectrophotometer (Perkin Elmer Spectrum 100). XRD analysis was also performed by using an X-ray diffractometer (Rigaku Miniflex II) to analyze the crystalline structure of AgNPs.

Particle morphology of AgNPs was determined by FESEM (FESEM Hitachi H-7100) at accelerating voltage of 10 kV, beam current 1 nA and typical measuring time of 7 sec. The purity of the AgNPs was determined by EDX analysis. For FESEM analysis one drop of reaction mixture containing AgNPs, was dried to form a smear over small piece of aluminium sheet. Further, detailed morphology of the synthesized AgNPs was explored by HRTEM analysis which was carried out on TECNAI 20 G2-electron microscope operated at accelerating voltage 200 kV. For HRTEM analysis, ultrasonically dispersed sample of AgNPs was layered on carbon coated copper grid through drop coating. HRTEM images have been processed using "Image J" software for calculation of average particle size distribution. The surface texture analysis was performed by AFM using NT-MDT working in the contact mode. AFM images have been processed using "NOVA" software. For the AFM analysis a single drop of colloidal AgNPs was spin coated over cover slip and dried under table lamp for two hour.

4.5.4 Microorganisms and inoculum preparation

The antimicrobial activity of AgNPs was evaluated against both Gram negative bacteria *E. coli,* (MTCC 1680) and Gram positive bacteria *S. aureus,* (MTCC 9886). The bacterial inoculums were prepared with the same procedure as per given in Part 3.2.13 of Chapter 1 of Section I.

4.5.5 Disc diffusion assay

The antimicrobial activity of the biologically synthesized AgNPs against both *S. aureus* and *E. coli* was also confirmed by the disc diffusion method as per guideline of National Committee for Clinical Laboratory Standards (NCCL standards, 1997). Briefly; the test organisms were grown in MHB at 35°C on a rotary shaker at 150 rpm for 24 h and thereafter bacterial density was adjusted to10^7 CFU/ml using sterile MHB. Bacterial inoculums were then spread-plated over the MHA plates. The discs (diameter 6 mm) soaked with 20 µL AgNPs solution of 50 ppm concentration, were gently transferred on to the surface of MHA plates. Control discs, separately inoculated with 20 µL of AES, $AgNO_3$ (8 mM) and PBS (10 mM) solution were also applied to the plate along with test disc. The plates were pre-incubated at 4°C for half an hour to facilitate uniform diffusion and further incubated at 37°C for 24 h and zone of inhibitions (ZOIs) were measured.

4.5.6 Assay for minimum inhibitory concentration (MIC) of AgNPs

MIC of AgNPs against both *E. coli* and *S. aureus* were determined by an amended broth macro-dilution method [Wendelin, 1997]. For MIC estimation, stock solutions of 30 different concentrations of AgNPs ranging from 1.0 µg/mL to 30.0 µg/mL were prepared in autoclaved MHB broth. Cotton plugged, sterile (13 x 100 mm) test tubes containing 2.0 mL of bacterial inoculum (10^7 CFU/mL) were arranged in two sets for each bacterial strain to cover the 30 different concentrations of AgNPs in duplicate. Thereafter, each test tube was individually inoculated with 2.0 mL of each concentration of AgNPs accordingly, thus final

volume of media in the flasks become 4.0 mL. This results to 1:2 dilution of AgNPs concentrations (i.e. 0.5-15.0 µg/mL) and of the bacterial inoculums (i.e. 5×10^6 CFU/mL). MHB with bacterial inoculum and MHB with AgNPs but without bacterial inoculum were taken as positive and negative control respectively. All test tubes were incubated at 35°C for 24 h. The microbial growth was indexed by measuring the optical density (O.D) at 600 nm by using U.V-visible spectrophotometer (Evolution 201, Thermo Scientific). The lowest concentration of AgNPs at which no visible growth observed even after 24 h was considered as MIC endpoint.

4.5.7 Cell viability test

E. coli and *S. aureus* were cultured in MHB for overnight at 37°C and then subcultured in fresh medium for 4h. Thereafter, the cells were collected by centrifugation and suspended in isotonic saline solution. Cell suspensions of both *E. coli* and *S. aureus* containing 10^7CFU/mL was individually supplemented with AgNPs adjusting concentrations equivalent to their MIC level. The cell viability of bacterial cells was evaluated by colony counting method in which 100 µL sample solution (10 fold diluted) was separately spread onto NA plates and incubated for 24 h at 35°C. NA plate inoculated with bacterial saline suspensions devoid of AgNPs was used as control. After incubation, colonies were counted and their number was compared with control plate to calculate the percentage viability of cells.

4.6 Results and Discussion

4.6.1 Primary verification AgNPs synthesis

Initial experiments were carried out in both direct sun light and dark condition, started with two sets of reaction mixtures. The visual appearance of reddish brown color in the reaction mixture was taken as the primary indication of biosynthesis of AgNPs. First set of reaction mixture, which was exposed to direct sunlight exhibits rapid color change from pale-green to reddish brown within 20 sec after inoculation of AES into $AgNO_3$ solution (*Fig. 4.3*). However, second set of

reaction mixture, which was kept at dark condition, did not attain the same degree of color change even after 12 h. This huge time lag clearly indicates the photo catalytic nature of AgNPs biosynthesis reaction. The appearance of color in reaction mixture was due to surface plasmon resonance of nanoparticles which arise through collective oscillations of free conduction electrons enforced by an interacting electromagnetic field [Mulvaney, 1996].

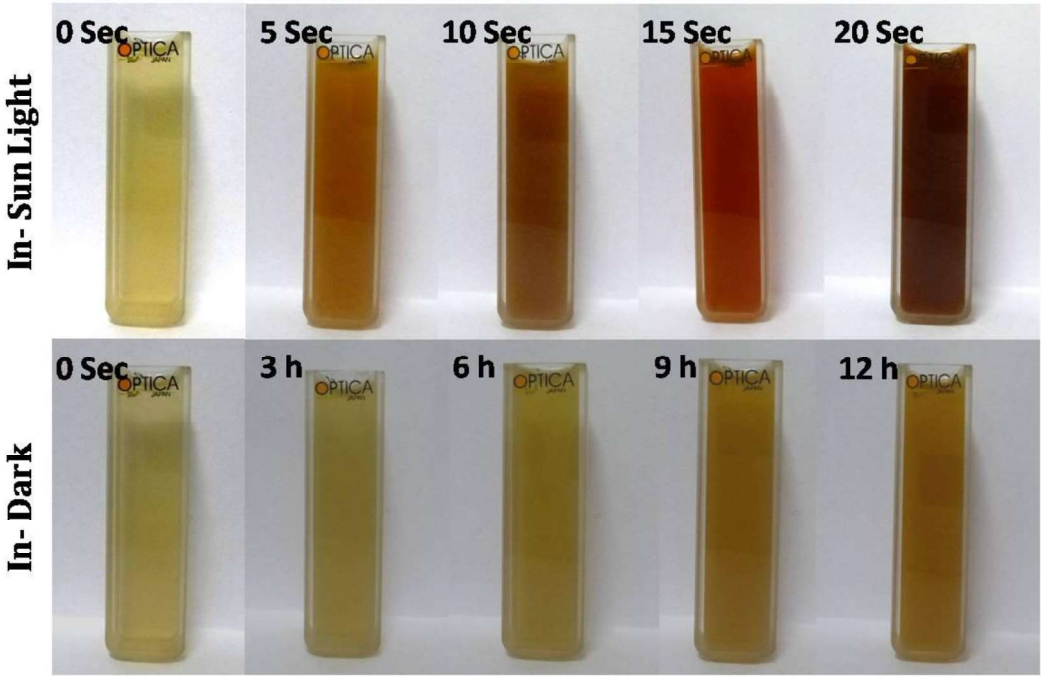

Fig. 4.3 Change in color of reaction mixture recorded at different time intervals in bright sunlight and in dark conditions.

To ascertain the formation AgNPs in both sets, the presence of characteristic SPR band in samples was screened through UV-visible spectroscopy between 300 nm to 700 nm after 1 min of reaction time. Samples from first set showed a sharp SPR band at 413 nm which is characteristic of AgNPs, whereas sample taken from second set after 1 min showed a very weak and undistinguished SPR band *(Fig. 4.4)*. This difference in SPR band intensity further confirms the photo-catalytic nature of light on biosynthesis of AgNPs for current system.

SPR band pattern and absorbance strongly influenced by material nature, surrounding media and shape-size of the nanoparticles [Jagtap and Bapat, 2013]. Mie's theory states that single SPR band in the UV-visible spectra indicate spherical shaped nanoparticles whereas multiple SPR bands indicate the presence of different shaped nanoparticles [Mie, 1908]. In present study, UV-visible spectra of reaction mixture showed single SPR band which indicate the spherical shape of synthesized AgNPs and it was further confirmed by FESEM and HRTEM analysis.

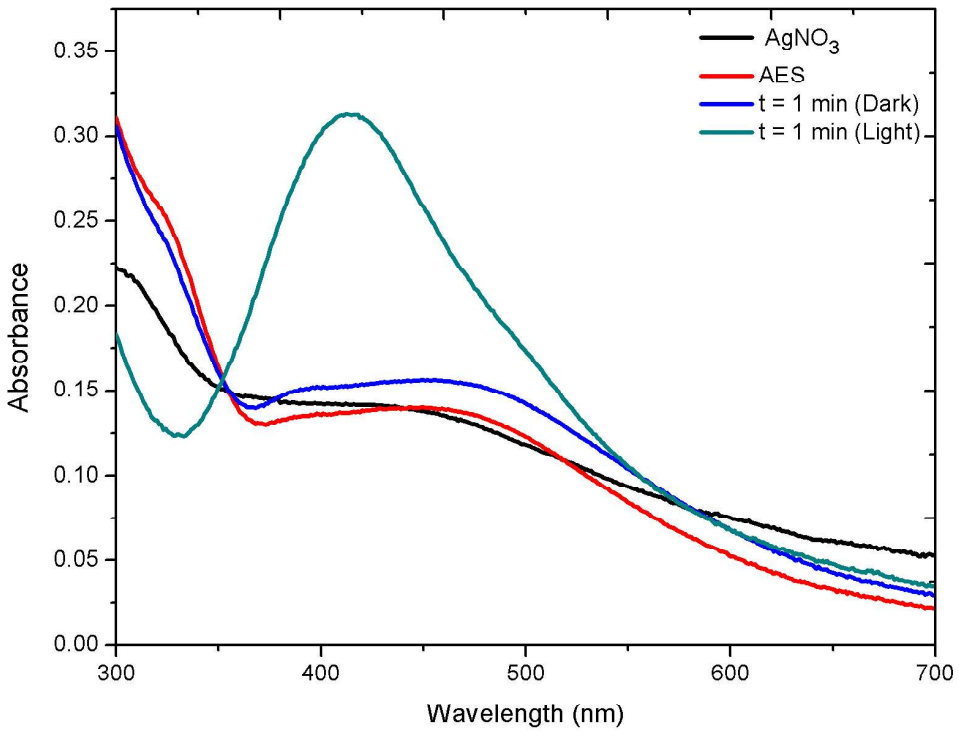

Fig. 4.4 U.V-Visible spectra for sunlight exposed reaction mixture and for reaction mixture kept at dark condition

4.6.2 Effect of sunlight exposure time on bio-synthesis of AgNPs

Sunlight exposure time was optimized by keeping the reaction mixture in direct sunlight under consistent observation. The samples were withdrawn at regular time interval of 5 min and analyzed through UV-visible spectroscopy to examine the equilibrium state and optimum reaction time for the process (*Fig. 4.5*).

The establishment of equilibrium was confirmed by monitoring the increment in SPR band intensity. Initially, it was observed that SPR band intensity continued to increase up to 35 min and thereafter no significant increment in band intensity with proceeding of time indicated the establishment of equilibrium. Therefore, 35 min of sunlight exposure time was considered as optimum for current photo induced biosynthesis of AgNPs.

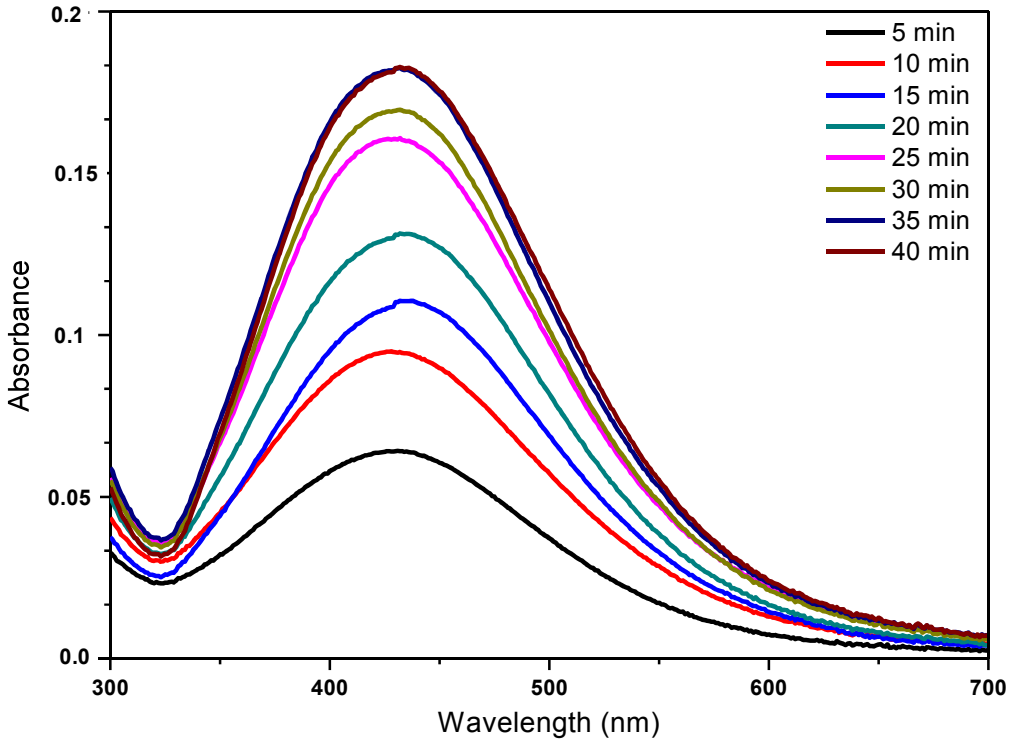

Fig. 4.5 UV–Visible absorption spectra of synthesized AgNPs recorded at different time (from 5 to 40 min) in direct sunlight exposure, conditions; $AgNO_3$ conc. 1 mM, AES inoculum dose 2.5% (v/v).

4.6.3 Effect of $AgNO_3$ concentration on AgNPs biosynthesis

The effect $AgNO_3$ concentration on the biosynthesis of AgNPs was investigated in the range of 1 mM to 10 mM at 2.5% AES inoculum dose and 35 min of sun light exposure time. *Fig. 4.6* represents the SPR bands for AgNPs at different $AgNO_3$ concentrations. It was observed that color of reaction mixture become darker with increase in $AgNO_3$ concentration in the solution for the fixed reaction time.

According to various prior scientific reports, the color of reaction mixture directly related with the size of nanoparticles [Mock et al., 2002]. Therefore it can be concluded that $AgNO_3$ concentration governs the particle size distribution for current system. Initial increase in $AgNO_3$ concentration from 1 mM to 8 mM results sharper and more intense SPR bands with regular blue sift in λ_{max} (424 nm to 410 nm) whereas further increase in $AgNO_3$ concentration from 8 mM to 10 mM results broader and less intense SPR bands. Increase in the band intensity indicates the increase in number of synthesized AgNPs per unit volume of reaction mixture whereas blue sift signifies the reduction in the size of AgNPs. Further at higher $AgNO_3$ concentration i.e. from 8 mM to 10 mM, broadening and reduction in SPR band intensity signified the synthesis of larger AgNPs in lesser number. Thus, 8 mM $AgNO_3$ concentration was chosen as optimal, in order to get smaller particle size with controlled growth for better antibacterial activity.

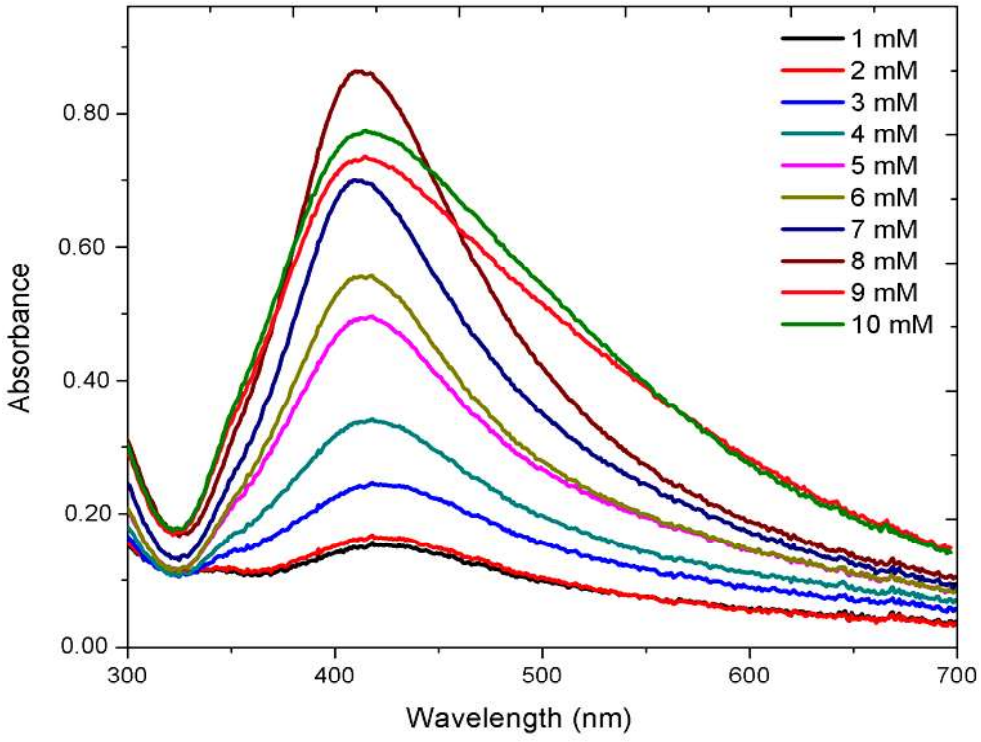

Fig. 4.6 UV–Visible absorption spectra of AgNPs, recorded as a function of variable $AgNO_3$ concentration varied from 1 mM to 10 mM, conditions; reaction time of 35 min in sunlight and 5.0 % (v/v) AES inoculum dose

4.6.4 Effect of AES inoculum dose on AgNPs

To optimize the inoculum dose, the experiments were conducted with varying AES inoculum dose (v/v) from 2.5% to 12.5% keeping other parameters constant at 35 min of exposure time and 8 mM $AgNO_3$ concentration. It was found that initially SPR band intensity increased with increase in AES inoculum dose from 2.5 % to 5.0 % thereafter it become broader and less intense with further increase in dose amount from 7.5% to 12.5 % (*Fig. 4.7*).

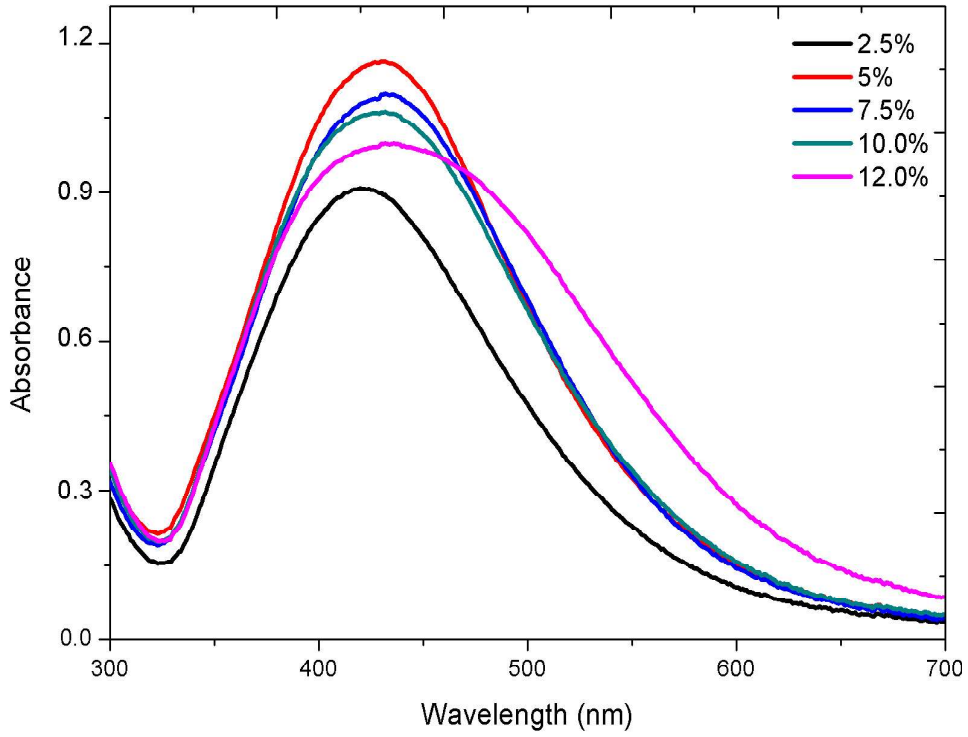

Fig. 4.7 UV–vis absorption spectra of AgNPs, recorded at different inoculum doses of AES varied from 2.5% to 12.5% (v/v), conditions; $AgNO_3$ concentration; 8mM and reaction time of 35 min in sunlight

According to the well established fact, a stable nuclei having size more than critical radius and sufficient amount of free metal ions are necessary for the formation of nanoparticles in the reaction mixture [Peng and Yang, 2009]. The nuclei with radius less than critical radius are unstable and redissolve in reaction mixture. At 2.5% of AES inoculum dose less number of nuclei were formed because of insufficient amount of reductant thus lesser number of nanoparticles were

synthesized resulting to less intense SPR band. At 5.0% AES inoculum dose higher number of stable nuclei formed than that of at 2.5% AES inoculum dose. This elevated nucleation at higher reductant volume would result in to synthesis of greater number of nanoparticles, which give rise intense SPR band. Further increase in AES inoculum dose from 7.5 % to 12.5 %, the SPR bands become broader and less intense with significant red sift in $\lambda_{max,}$ (from 419nm to 427 nm) which indicates the synthesis of large sized AgNPs in less number. This is because at very high AES inoculum dose nucleation was so rapid that most of nuclei formed were unstable due to their size smaller than critical radius thus redissolved in reaction mixture. During this process only few number of nuclei remains stable thus lesser number of nanoparticles were synthesized. The dissolved unstable nuclei provide extra free Ag^{+} ions for growth of stable nuclei which results in to overgrowth thus larger sized AgNPs were synthesized. On the basis of these results, 5.0% (v/v) AES inoculum dose was considered as optimum for further experimentation.

4.6.5 Characterization and stability of AgNPs

AgNPs synthesized at optimized process parameters were collected and further characterized through FESEM, EDX, HRTEM, AFM, XRD, and FTIR, analysis.

For the FESEM analysis, one drop of fresh reaction mixture having synthesized AgNPs was put over the thin sheet of the aluminium and dried in shade to form a thin smear. FESEM images (*Fig 4.8a*) showed the discrete distribution of monodispersive spherical shaped AgNPs.

The purity and elemental composition of AgNPs was analyzed through FESEM equipped EDX detector. A prominent spectral signal of silver at 3 keV was observed in energy dispersive spectra of EDX, which corresponds to optical absorbance of AgNPs due to SPR (*Fig. 4.8b*). Spectral signals for oxygen and carbon were also recorded due to presence of the biological in the vicinity of AgNPs

[Jayaseelan et al., 2013]. The peak of aluminium in spectra was due to aluminium sheet on which sample smear was made.

HRTEM analysis was performed to explore detailed surface morphology of biosynthesized AgNPs. The HRTEM image (*Fig 4.8c*) revealed the abundance of roughly spherical shaped AgNPs with size ranging from 1 nm to 35 nm. The selected area electron diffraction (SAED) pattern of AgNPs is shown in *inset of Fig. 4.7c.* The bright circular rings in SAED pattern confirmed the crystalline nature of synthesized AgNPs. A size distribution histogram (*Fig. 4.8d*) of AgNPs corresponding to HRTEM image represented that majority of nanoparticles were in range of 5 nm to 15 nm having average size distribution of 12.46 nm. AFM technique was used to study the surface characteristics of the biosynthesized AgNPs. Fig. 3e and 3f represented the 2D and 3D topographical view of AgNPs. The average roughness of the sample and area peak to valley height was 40.36 nm, and 31.98 nm respectively. The uneven surface morphology was due the presence of both individual and agglomerated AgNPs.

XRD data of synthesized AgNPs were collected at wide angular range of $20° \leq 2\theta \leq 80°$ and the crystalline nature of silver nanoparticles was confirmed by the analysis of XRD pattern as shown in *Fig. 4.9a.* XRD pattern of AgNPs showed four distinct diffraction peaks at $2\theta = 38.21°$, 43.23°, 64.66° and 77.32° which can be indexed to the (111), (200), (220) and (311) reflection planes of face centred cubic (fcc) crystal lattice of metallic silver. Peaks were well matched with standard diffraction data of AgNPs (JCPDS file no.893722) shown in Fig. *4.9b.* Apart from these distinct peaks, XRD pattern also exhibited some other minor peaks. These minor peaks are due to the organic compounds which are present in the herbal extract and responsible for silver ions reduction and stabilization of resultant nanoparticles [Roopan et al., 2013].

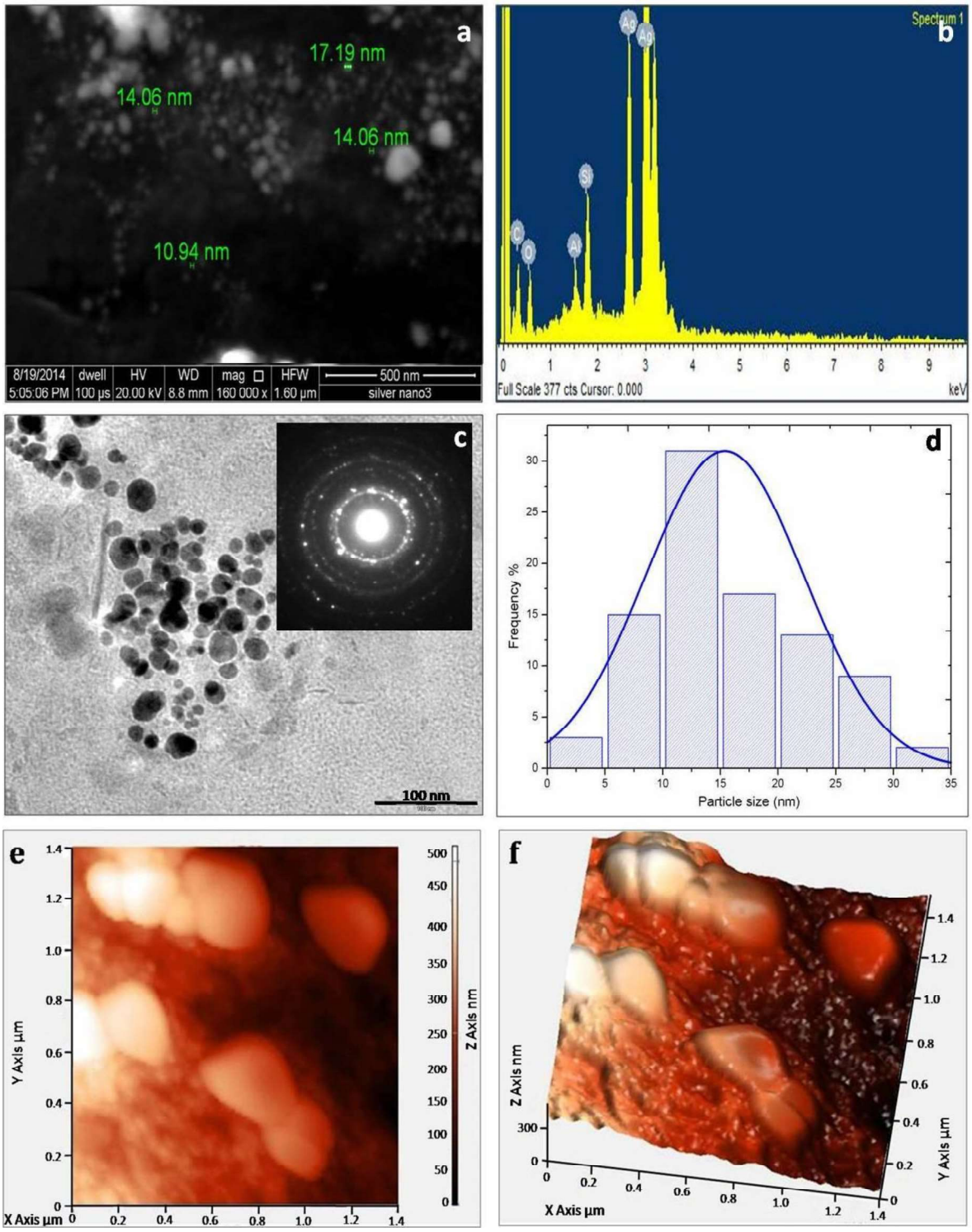

Fig. 4.8 (a) FESEM images of AgNPs synthesized by 5.0 (v/v) % AES, 8 mM $AgNO_3$ and 35 min of sunlight exposure time (b) EDX spectrum of AgNPs obtained from optimization. (c) HRTEM images of optimized AgNPs, SAED pattern of crystalline AgNPs (inset), (d) AgNPs Histogram. (e) AFM of images showing lateral view of AgNPs (f) AFM of images showing 3D view of AgNPs

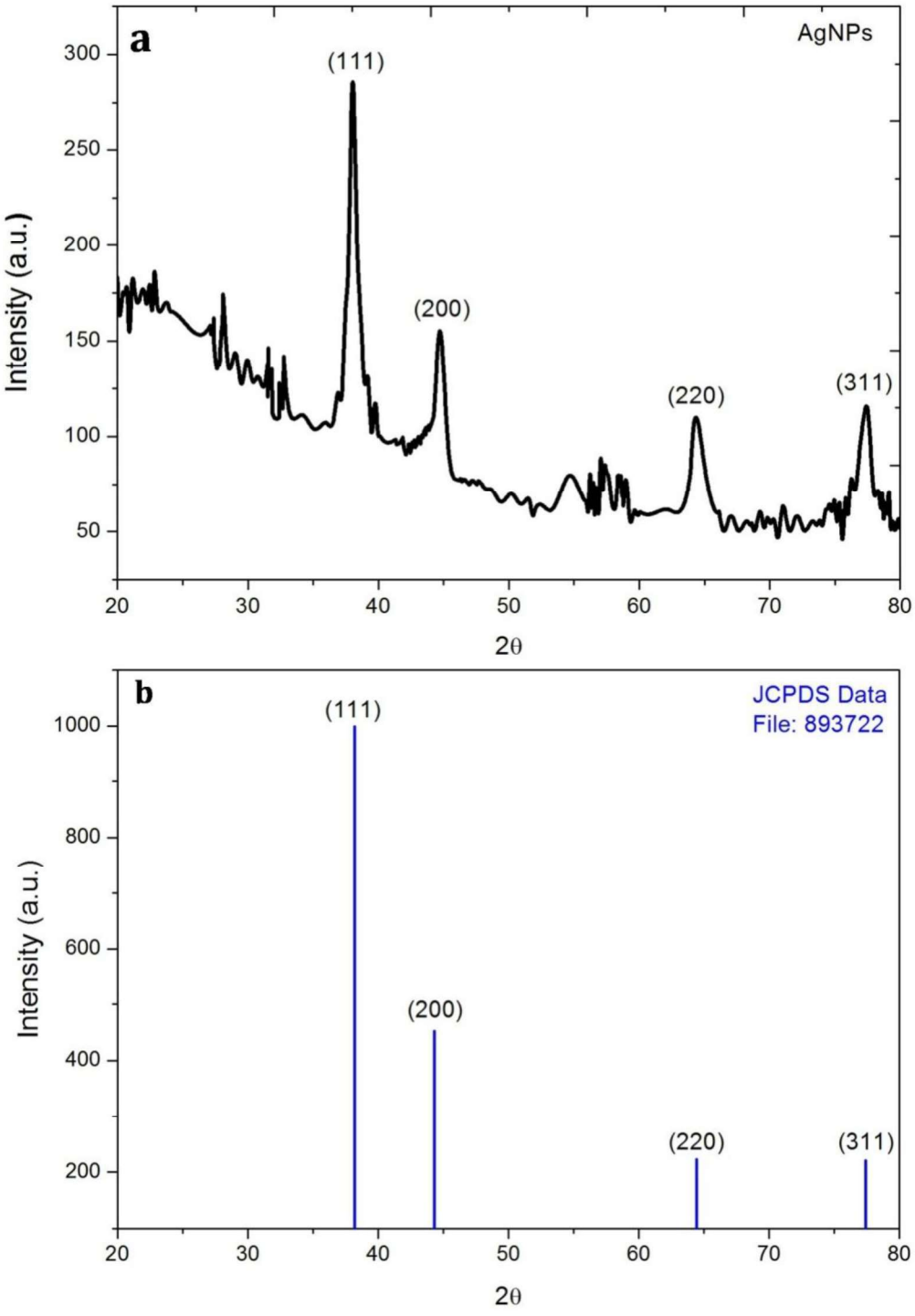

Fig. 4.9 (a) X-ray diffraction pattern of synthesized AgNPs. (b) JCPDS data (File No.893722) for comparative analysis of XRD pattern of AgNPs.

FTIR analysis of both AES and AgNPs was carried out to investigate the possible biomolecules in AES responsible for the synthesis and stabilization of AgNPs. IR spectra *(Fig. 4.10)* of AES showed prominent bands at 3420.27, 1633.27, 1324.29 and 1019.12 cm^{-1}. Broad band around 3200-3500 cm^{-1} corresponds to –OH groups of tannin, flavanoides (phenolic compounds), glucose and –NH stretching of the proteins. Band at 1633.27 cm^{-1} represent primary amines (1°, 2°) and amide linkage of proteins whereas bands at 1324.29 & 1019.12 cm^{-1} stands for C=O symmetric stretching of –COOH and –C–O stretching vibrations of ether as well as alcoholic groups respectively [Bai and Abraham, 2002; Huang et al., 2009; Nakano et al., 2001; Velmurugan et al., 2013]. In comparison with the IR spectrum of AES, the spectra of AgNPs showed a shifting in following peaks: from 3420.27 to 3470.14, 1633.27 to 1631.46, 1324.29 to 1368.11 and 1019.12 to 1004.34 cm^{-1} respectively. These findings indicated the involvement of hydroxyl, carboxyl, amino and amide groups of phyto-chemicals present in AES for the biosynthesis of AgNPs. These groups can majorly be contributed by tannins, flavanoids, phenolic compounds and proteins present in AES [Mithraja et al., 2011]**.**

4.6.6 Stability of synthesized AgNPs

Stability of AgNPs, synthesized at optimum process parameters, was also monitored and results are shown in *Fig 4.11*. To examine the stability of AgNPs, both the visual precipitation and change into SPR band intensity was taken in account. The AgNPs were found to be stable for 1 week with mild appearance of turbidity in the samples. After 7 days, turbidity of sample gradually increased and finally encountered the precipitation of AgNPs at the bottom of the flask, which might be due to over growth and agglomeration of AgNPs with passage of time.

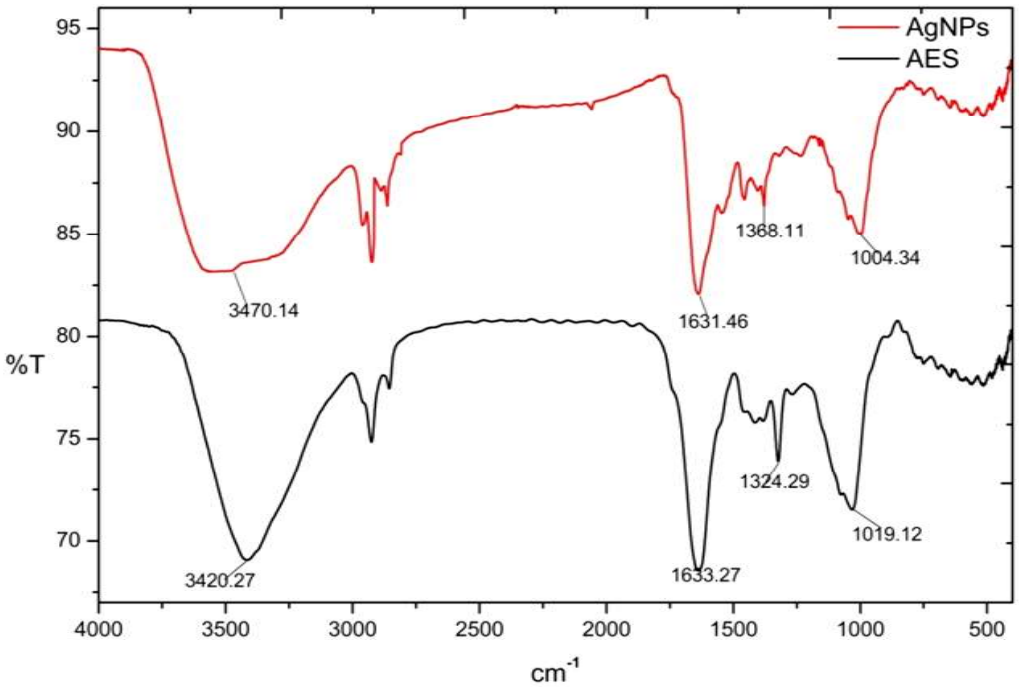

Fig. 4.10 Typical FTIR spectra of the AES and AgNPs

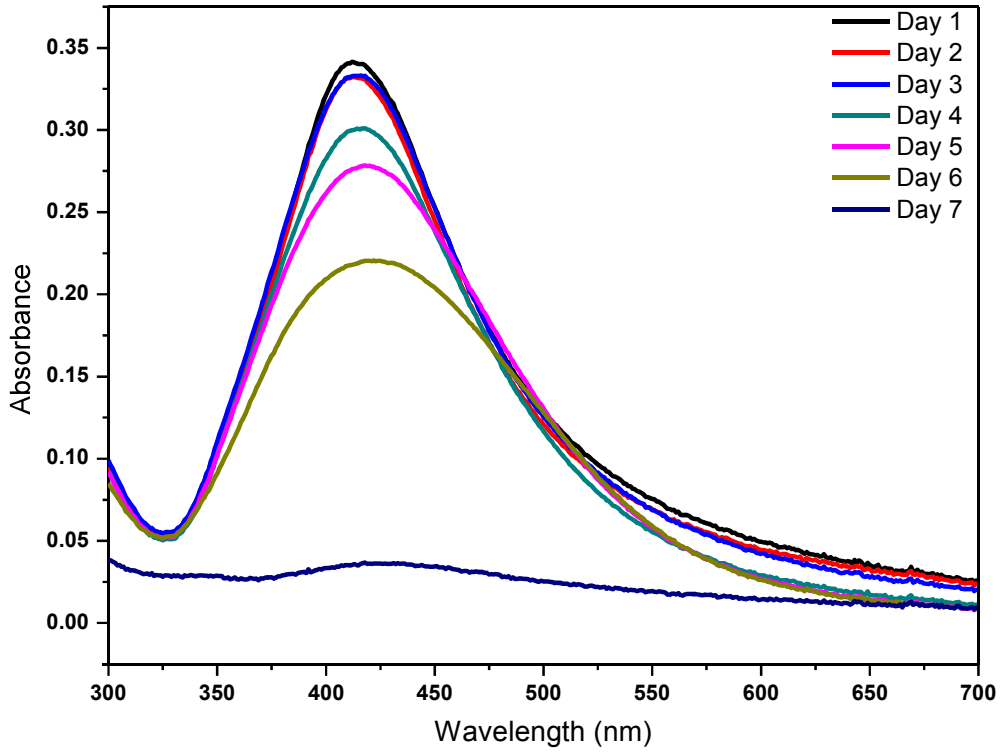

Fig. 4.11 U.V-Visible spectra of AgNPs showing stability of AES synthesized AgNPs up to 7 days of incubation period

4.6.7 Biosynthesis mechanism of AgNPs using AES

We have also proposed a probable mechanism of AgNPs synthesis on the basis of phytochemical constituents of AES, photocatalytic effect of sunlight along with FTIR analysis of AES and AgNPs. Presence of alkaloids, flavonoids, phenols, tannins, sugars, proteins and many other phytochemicals in herbal extract *Salvinia molesta* have already been reported by many researchers through phytochemical analysis [Mithraja et al., 2011, Devi et al., 2015]. Tannins and flavonoids are well reported effective reducing agents for AgNPs synthesis, whereas proteins, glucose and some other phytochemicals can act as capping agent [Bulut and Ozacar, 2009; Mathur, 2014]. The probable reaction mechanism is presented as schematic diagram in *Fig 4.12a*. Multiple hydroxyl groups present in tannin or other phenolic phytochemicals of AES may participate in the reduction reaction. Ag^+ mediated oxidation of tannin from its enol form to quinonoid form lead to subsequent reduction of Ag^+ ions into AgNPs. Ag^+ first oxidizes tannin and forms an intermediate silver complex and then finally silver ion of this complex reduced to Ag^0 by accepting an electron from a suitable electron donor leaving tannin into its quinonoid form. Many flavin binding proteins, terpenols, flavonoides and other phytochemicals are photo responsive; they either itself can easily donate the electrons in presence of sunlight or can induce other compounds to do the same [Gade et al., 2014]. This fact is also supported by the results of our study which indicate the photo-catalytic nature of current system. Removed hydrogen from tannin may also act as a source of electron thus tannins can itself act as a reducing agent. Reducing sugars of AES can also provide an alternative reduction route. Proteins, sugars or some other phenolic compounds present in AES can act as stabilizers for AgNPs *Fig 4.12b*. This prediction can be evident from the IR analysis of AES and AgNPs, which clearly indicated the involvement of –OH and $–NH_2$ groups in synthesis and in stabilization of AgNPs.

(a)

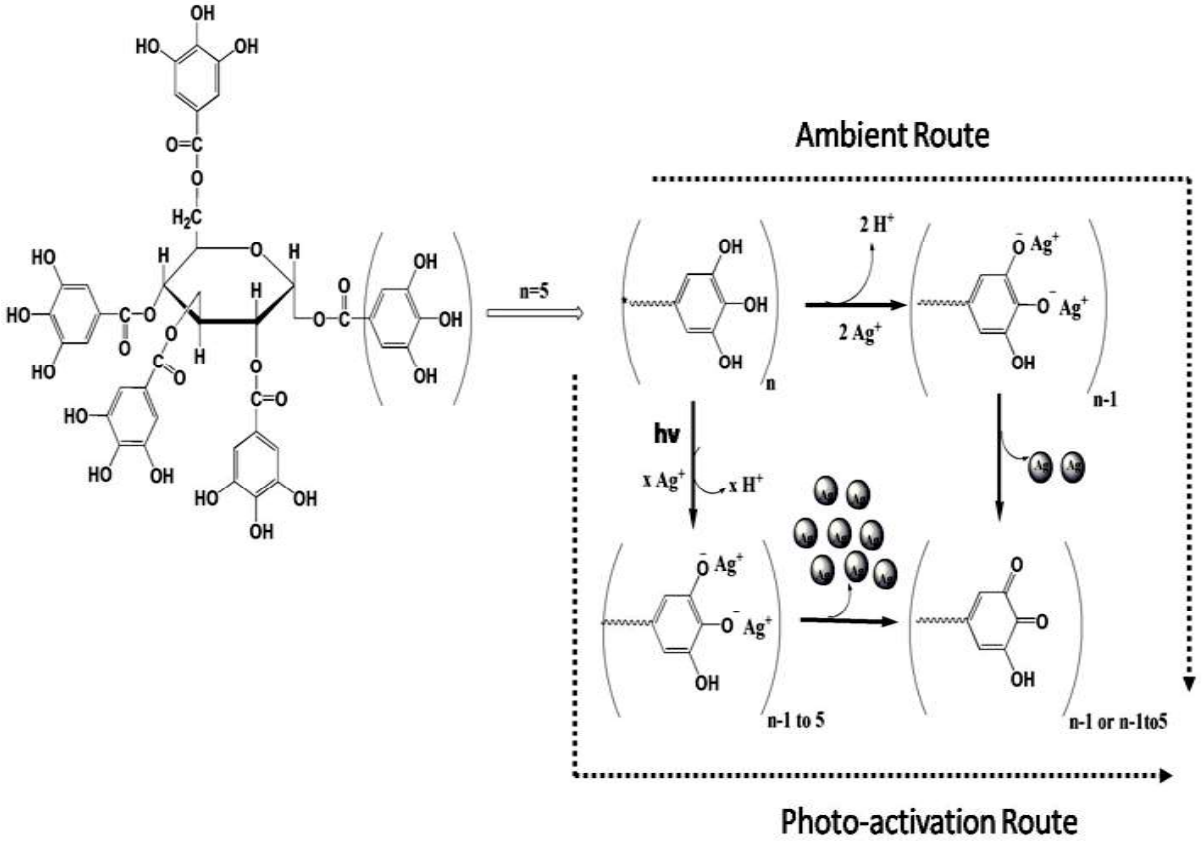

(b)

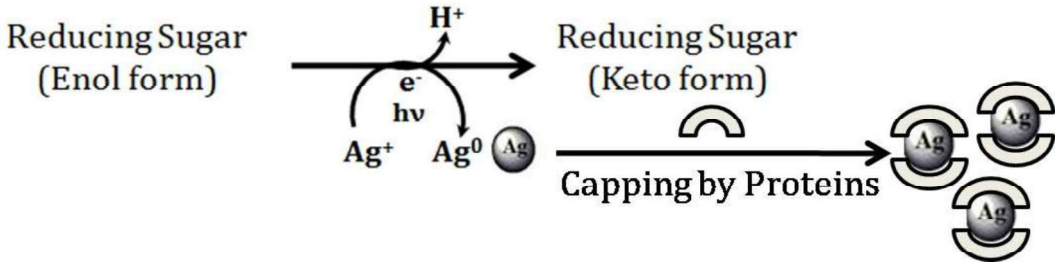

Fig. 4.12 Schematic representation of probable mechanism for; (a) biosynthesis of AgNPs using AES through both photo-activated and ambient route i.e. at normal lab conditions, tannin was considered as bioreductant (b) alternative reduction route through reducing sugars of AES and stabilization of synthesized AgNPs through protein capping

4.6.8 Disc diffusion assay and minimum inhibitory concentration

The antibacterial efficacy of synthesized AgNPs was evaluated against *Staphylococcus aureus* and *E. coli* through disc diffusion methodology. Thereafter, MIC of AgNPs for both bacterial strains was estimated though macro-dilution method. ZOIs around the discs inoculated with suspensions of AgNPs, AES, and 8 mM $AgNO_3$ solution are shown in *Fig. 4.13(a,b)* whereas *Table 4.2* showed the diameter of ZOIs in each case. The results clearly indicate that the AgNPs had significant antibac terial effects on tested bacteria of both gram classes. AgNPs were found to be more effective against *E. coli* (Gram negative) than that of *Staphylococcus aureus* (Gram positive). The reason of greater susceptibility of negative bacteria for AgNPs may be associated with the fact that, Gram negative bacteria pose weaker cell wall due to less peptidoglycan content as compare to Gram positive bacterial cell wall [Chaloupka et al., 2010]. These findings are in agreement with many previous reports [Kim et al., 2007; Gurunathan et al., 2014; Hungund et al., 2015].

Minor ZOIs were also observed around the discs containing AES and AgNPs. $AgNO_3$ showed mild antibacterial activities due to interaction of its free silver ions with thiol group in vital enzymes of bacteria whereas herbal extracts poses antimicrobial activity due to bioactive activities of their phytochemicals. Three mechanisms commonly accepted about the mode of action of AgNPs,: (1) direct disruption of cell wall and plasma membrane (2) Reactive Oxygen Species (ROS) mediated toxicity (3) Interference with ATP metabolism as well as DNA replication [Jones and Hoek, 2010]. It is also relevant to mention here that smaller AgNPs (~10 nm) shows greater antibacterial activity as compare to larger nanoparticles because smaller AgNPs produces electronic effect after interacting with bacteria [Raimondi et al., 2005]. Because the average size of synthesized AgNPs reported in the current study was around 10 nm which makes them suitable for the

antibacterial application. After primary confirmation of antimicrobial activity of AgNps through disc diffusion assay, their MIC values for test organisms were also estimated via macro dilution method because MIC value provides more definite quantitative data about antimicrobial efficacy. MIC for *E. coli* and *S. aureus* was found to be 10.50 µg/mL and 13.0 µg/mL. Lower MIC value for *E. coli* indicates its getter susceptibility for AgNPs. These findings further support the results of antimicrobial assay. The reason behind lower MIC value is same as discussed above for the getter susceptibility of Gram –ve bacteria for AgNPs.

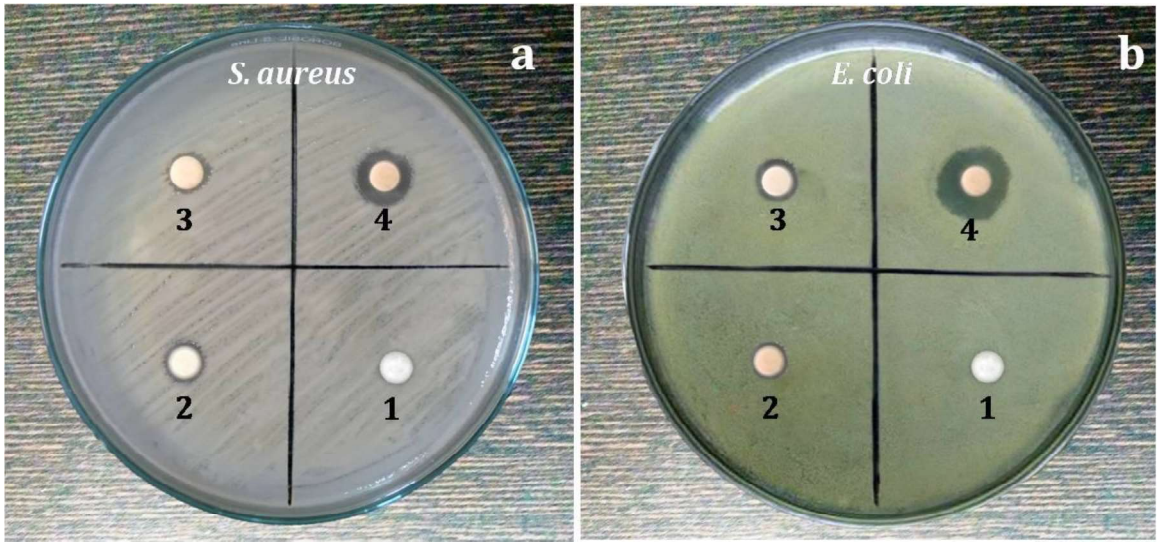

Fig.4.13 Antimicrobial efficacy of synthesized AgNPs against; (a) *Staphylococcus aureus* (Gram +ve) (b) *E. coli* (Gram -ve). Disc (1) Buffer solution, (2) AES (3) $AgNO_3$ and (4) AgNPs.

Table 4.2 *Antimicrobial activity of Salvinia molesta (AES), $AgNO_3$ solution and AgNPs against E. coli and S. aureus. Phosphate buffer saline was used as control*

Disc	Applied Substance (20 µL)	Zone of inhibition (ZOI) in mm	
		Eischherichia coli	*Staphyloccocus aureus*
1	Buffer Solution (Control)	0	0
2	AES	8	7
3	$AgNO_3$ (8 mM)	11	10
4	AgNPs (50 ppm)	21	16

4.6.9 Cell Viability test

Time dependent antibacterial behavior of AgNPs against both the test microorganisms i.e., *E. coli* and *S. aureus,* was evaluated through cell viability test. The cells of *E. coli* and *S. aureus* (10^7cells/ml) were incubated in separate MHB media having AgNPs concentration of 10.50µg/mL and 13.0 µg/mL respectively. Cell viability of both microorganisms was monitored at regular time interval through colony counting method and the results are presented in *Fig. 4.14.*

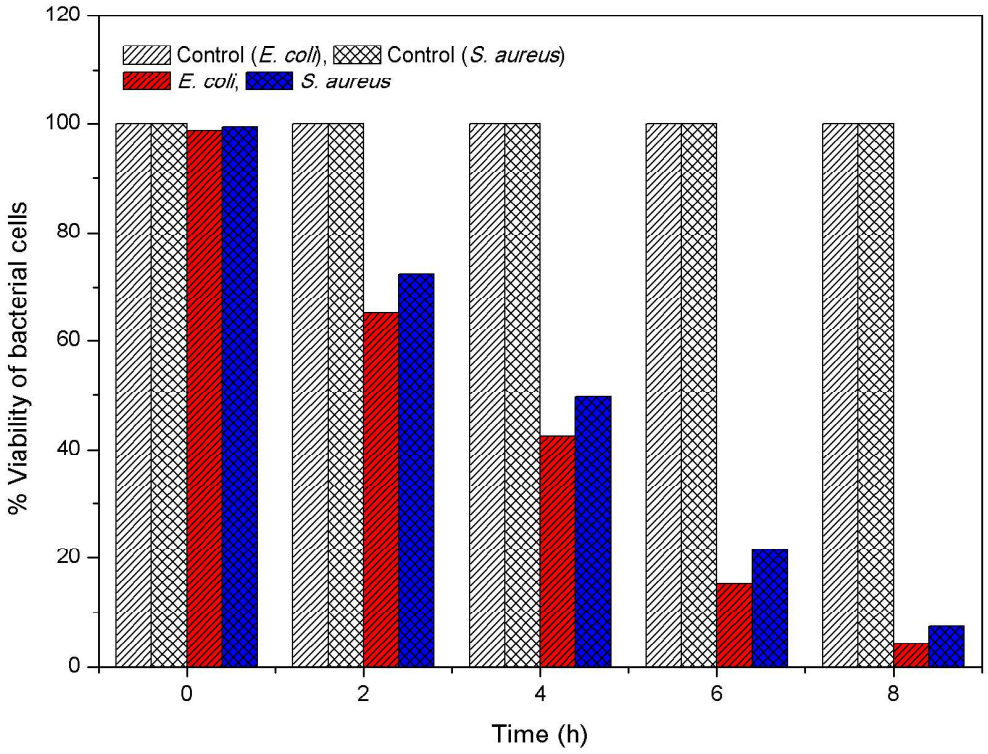

Fig 4.14 Cell-viability test: decrease in cell viabilities of *E. coli* and *S. aureus* (10^7 colony forming units/mL) when treated with AgNPs (conc. equivalent to MIC) at 37 °C for 8 h

The loss of cell viability of *E. coli* and *S. aureus* was counted at bi-hourly intervals. *E. coli* cells incubated with 10.50 µg/mL AgNPs showed percentage loss of cell viability; 1.2, 34.8, 57.5, 84.8 and 95.8 % after 0, 2, 4, 6 and 8 h, respectively. *S. aureus* cells incubated with 13.0 µg/mL AgNPs showed percentage loss of cell viability; 0.6, 27.6, 50.4, 78.5 and 92.6 % after 0, 2, 4, 6 and 8 h, respectively. Initial

4 h showed rapid killing of microorganisms, which indicated fast the better affectivity of AgNPs against test bacterial strains. There was no loss of cell viability was observed in control samples of *E. coli* and *S. aureus.*

4.7 Conclusion

In current study a very simple one step green route have been developed for the synthesis AgNPs at ambient environmental conditions, using AES. The developed photo-catalytic methodology was found to be very swift and efficient to synthesize the AgNPs within 20 seconds without using any instrument, chemical reductant or external energy supply. After process optimization; the optimum conditions were found as; 8 mM $AgNO_3$ concentration, 5.0 % (v/v) of AES inoculum dose and 35 min of sun light exposure time. Synthesized AgNPs were crystalline, spherical and small, having average size distribution of 12.46 nm. On the basis of IR results and previously reported phytochemical analysis of *Salvinia molesta*, a probable mechanism for synthesis of AgNPs was proposed. Polyphenols and proteins were concluded as possible bioreductant and stabilizing agents respectively. Antibacterial studies reviled the better efficacy of AgNPs against Gram negative bacteria as compare to Gram positive bacteria.